SUPPLEMENTARY INFORMATION

Tuning the anisotropic facet of Cu_2O single-crystals for photocarrier spatial segregation

Shuo Tian,[a] Yunsen Wang,[a] Shuyun Chen,[a] Zhichao Yu,[a] Di Wu,[a] Jiao Qin,[a] Dianyong Tang*[b] and Dianping Tang*[a]

[a] Key Laboratory for Analytical Science of Food Safety and Biology (MOE & Fujian Province), Department of Chemistry, Fuzhou University, Fuzhou 350108, P. R. China

[b] Chongqing Key Laboratory of Kinase Modulators as Innovative Medicine, College of Pharmacy (International Academy of Targeted Therapeutics and Innovation), Chongqing University of Arts and Sciences, Chongqing 402160, P. R. China

Experimental Procedures

Materials and Reagents. Copper (II) Chloride Dihydrate ($CuCl_2 \cdot 2H_2O$, 99%), sodium hydroxide (NaOH, 96%), ascorbic acid ($C_6H_8O_6$, 99.7%), polyvinyl pyrrolidone (PVP, $(C_6H_9NO)_n$, M.W. 24000), and sodium sulfate anhydrous (Na_2SO_4, 99.5%) were purchased from Aladdin Pharmaceutical Company (Shanghai, China) and used without further purification. Antibodies were purchased from Keyue Biotech. Inc. (Beijing, China). Carcinoembryonic antigen (CEA) was purchased from Zhengzhou Biocell Biotech. Co., Ltd. (Zhengzhou, China). Carcinoembryonic antigen (CEA) ELISA kit was obtained from Wuhan Cusabio Biotech. Inc. (Wuhan, China, https://www.cusabio.com/). Phosphate buffered saline (PBS) consisted of 0.1 M NaH_2PO_4, 0.1 M Na_2HPO_4, 0.1 M KCl (pH 7.4). Ultrapure water was treated by a Millipore water purification system (Z18 M Ω, Milli-Q, Millipore).

Experimental Characterization. The scanning electron microscope (SEM) characterizations were performed on the TESCAN MIRA4 field emission scanning electron microscope. The nanoparticles were characterized by using transmission electron microscopy (TEM, FEI Talos F200s). UV-vis absorption spectra were recorded by the Infinite M200 Pro NanoQuant (Tecan, Switzerland). The portable measurement fixture was produced by the 3D printer of Formlabs Co., Ltd. X-ray photoelectron spectroscopy (XPS) was recorded on a K-Alpha X-ray photoelectron spectrometer (Thermo Fisher Scientific Co., USA). The X-ray diffraction (XRD) patterns were recorded by a Bruker D8 Advance X-ray diffractometer with Cu Kα lines in the range of 2θ from 20 to 80°. The electron paramagnetic resonance (EPR) spectra were recorded on a Bruker EMXplus X-band. The PEC measurements were performed with a microelectrochemical workstation (Shenzhen Haoyang Science and Technology Ltd).

Testing of ultraviolet-visible diffuse reflectance spectra. The method for testing ultraviolet-visible diffuse reflectance spectroscopy (UV-Vis DRS) is the integrating sphere technique.[1] Light emitted from the source is processed before entering the sample. It passes through an integrating sphere with an inner wall coated with MgO (or $BaSO_4$ etc.), where the reflected light from the sample surface is collected and then projected onto a detector (a photomultiplier tube or photodiode). This generates an electrical signal, which is recorded as a function of wavelength on a chart recorder, forming a spectral curve. Generally, an integrating sphere accessory can be fitted to a UV-vis

spectrophotometer to determine the UV-Vis DRS. According to the Kubelka-Munk function, the absorbance could be calculated as follows:[2]

$$F(R_\infty) = K/S = \frac{(1 - R_\infty)^2}{2R_\infty}$$

$$R = R_\infty(sample)/R_\infty(standard)$$

$$A = \lg(1/R)$$

where R_∞ represents the reflectance of an infinitely thick sample; K stands for he absorption coefficient; S is the scattering coefficient; A is the absorbance; R refers to the actual measured reflectance.

Calculation of Built-In electric Field Intensity. According to Kanata-Kito model, the built-in electric field of materials could be calculated as follows:[3]

$$F_s = (-2V_s\rho/\varepsilon\varepsilon_0)^{1/2}$$

where F_s represents the intensity of the built-in electric field; V_s stands for the surface photo-voltage; ρ is the surface charge density, which will be obtained by the integral value of the current density; ε is the dielectric constant measured by the vector network analyzer; ε_0 refers to the vacuum dielectric constant. The surface charge density was obtained via the integral of the transient anodic photocurrent peak. The surface voltage was measured via the open-circuit potentials.

DFT Calculation. Density function theory (DFT) calculations based on the first principle were analyzed using Materials Studio software.[4–6] The generalized gradient approximation (GGA) method was chosen for the exchange-correlation energy approximation method, and the PBE (Perdew-Burke-Ernzerhof) function was selected as the gradient function. The plane-wave pseudopotential method was used to realize the DFT-related calculation. The selection of suitable high symmetry points k describing the Brillouin zone was based on the Monkhorst-Pack method. The convergence accuracy was set to less than 0.05 eV $Å^{-1}$ for the residual force on each atom and a convergence tolerance of 10^{-7} for the energy difference of two consecutive self-consistent calculations.

The structure of Cu_2O {100} and {111} facets was built based on a 3 × 3 superunit with the original structural atom of Cu_2O. The adsorption energy (E_{ads}) between the catalyst slab and adsorption molecules was calculated by the following equation:

$$E_{ads} = E_{total} - E^*_a - E_{slab}$$

Where E_{total}, E_a, and E_{slab} are the total energy of the optimized adsorbate on the catalyst surface, the energy of adsorption molecules, and the catalyst surface, respectively, and all of the energies are in the units of eV.

Design and Construction of 3D Printed Support Devices. The integrated photoelectrochemical microcell device was supported via one-step direct 3D printing.[7] The execution procedure of the stereo model was performed with the assistance of a Form2 3D printer (Formlabs, USA). The photosensitive resin of choice was clear resin (FLGPCL04), purchased from a local distributor. After printing, additional liquid resin was cleaned with isopropyl alcohol, and the kit was stored in a cool place.

Preparation Method of Cu_2O Modified Fluorine-doped Tin Oxide (FTO). (i) Wash the new FTO glass with ethanol and deionized water and dry at room temperature; (ii) Bonded with waterproof scotch tape with a radius of 3 mm, the cleaned FTO is treated with a punch; (iii) the aqueous suspension of Cu_2O prepared above was thrown on the surface of FTO and dried at room temperature; and (iiii) measurement of photocurrent in a cell made by an electropotentiostat.

Measurement of Photoelectrochemical (PEC) Properties. The electrochemical and PEC properties were investigated on the CHI-660E electrochemical workstation. The working electrolyte utilized was 0.1 M Na_2SO_4 with a standard three-electrode system for the synthesized samples. The Ag/AgCl and Pt wire served as the reference and counter electrodes. Synthesized x-Cu_2O photoelectrodes were used as working electrodes. No bias was applied, except as specially indicated. The PEC measurements were carried out under visible-light illumination (Xe lamp $\lambda > 400$ nm; power intensity: 500 W). The monochromatic light irradiation was adopted Xe lamp equipped with 400 nm, 450 nm, 500 nm, 550 nm, 600 nm and 650 nm filters. The optical power meter (Thorlabs) was utilized to evaluate the power density of each wavelength. The transient photocurrent response was achieved by light shutter. The cycles were all 20 seconds with 10 seconds for illumination and 10 seconds for switching off. Mott-Schottky (MS) plots were obtained at a frequency of 2000 Hz with an amplitude of 10 mV without illumination.

Preparation of mAb_1-Coated Microplate. Monoclonal antibodies to CEA were prepared and bonded in microtiter plates as follows. The purchased mAb_1 (50 μL per well, 10 μg mL^{-1}) was added

to a high-binding 96-well microplate containing sodium carbonate buffer (0.05 M, pH 9.6), and then incubated for 24 h at 4 °C. A plastic film is wrapped over the microplate to prevent evaporation of the liquid. The completed incubated microplates were removed and washed three times with PBS (pH 7.4) buffer containing 0.05 % Tween 20 (v/v). This was followed by incubation for 1 h by adding closure buffer (300 μL of PBS solution per well (10 mM, pH 7.4) including 1.0 wt % BSA). The aforementioned prepared microtiter plates were prepared for the CEA assay. Finally, the treated plates were stored at 4 °C and used as soon as possible.

Preparation of GOx/pAb$_2$-Conjugated AuNP (GOx-AuNP-pAb$_2$). GOx-AuNPs-pAb$_2$ conjugates were prepared according to our previous reports. Firstly, gold colloids (5.0 mL, 5.0 ng mL^{-1}) were adjusted to pH 9.5 by using 0.1 M Na_2CO_3 aqueous solution. Then, 200 μL of GOx (0.5 mg mL^{-1}) and 50 μL of pAb$_2$ (0.5 mg mL^{-1}) were injected into colloidal gold nanoparticles and gently shaken for 30 min at room temperature on a shaker (MS, IKA GmbH, Staufen, Germany). 100 μL of polyethylene glycol (1.0 wt %) was added into the suspension. The mixture was further incubated for 12 h at 4 °C. Finally, GOx-AuNP-pAb$_2$ conjugates were obtained by centrifugation at 4 °C (10 min, 13000 g), and dispersed in 1.0 mL of 2 mM sodium carbonate solution ($C_{[AuNP]} \approx 25$ ng mL^{-1}) containing 1.0 wt % BSA and 0.1 wt % sodium azide, pH 7.4, and stored at 4 °C for further use.

Monitoring of Human Serum Samples and Interlaboratory. Before measurement, these collected human serum samples from Fujian Provincial Hospital (Fuzhou, China) were initially centrifuged for 5 min at 4 °C with 5,000*g* (centrifugal force) to remove any impurities and macromolecules that might be present. Thereafter, the obtained supernatant fluids were determined using the developed PEC immunoassay and the commercialized human CEA ELISA kit, respectively. The high-concentration CEA samples were diluted with PBS (10 mM, pH 7.4). All the experiments were performed according to the Guidelines of Fuzhou University (China) and approved by the ethics committee at Fuzhou University (China). Informed consents were obtained from human participants of this study. CEA levels in these specimens were calculated based on the calibration curve in Fig. 5B, referring to the obtained photocurrents per sample. For comparison, these samples were determined by commercialized available human CEA ELISA kits as the reference. The method accuracy and interlaboratory validation were evaluated by using a Student's t-test method.

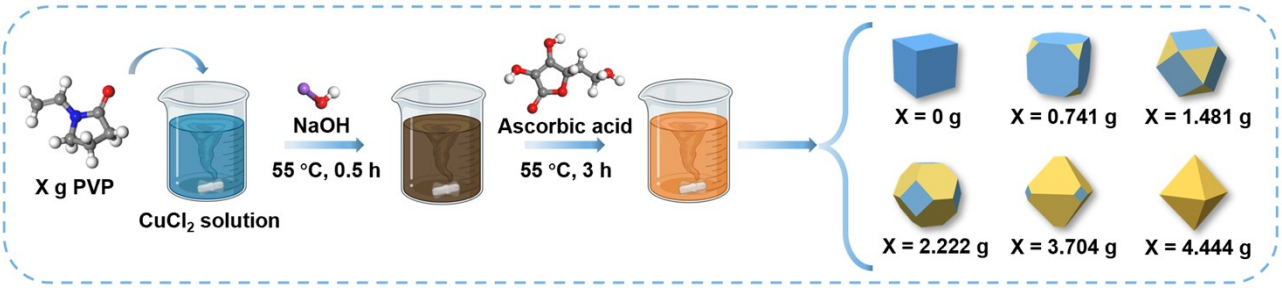

Fig. S1. Schematic of the synthesis of Cu_2O with different crystal facets exposed.

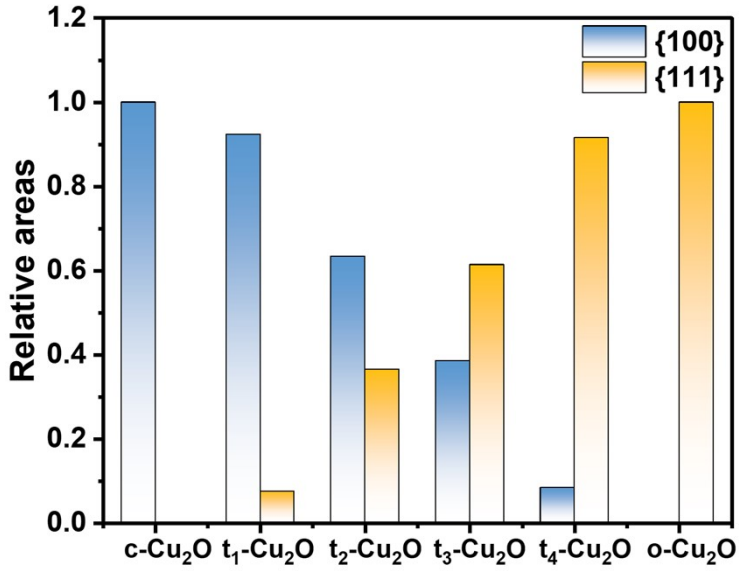

Fig. S2. The relative areas of different exposed facets in Cu_2O crystals.

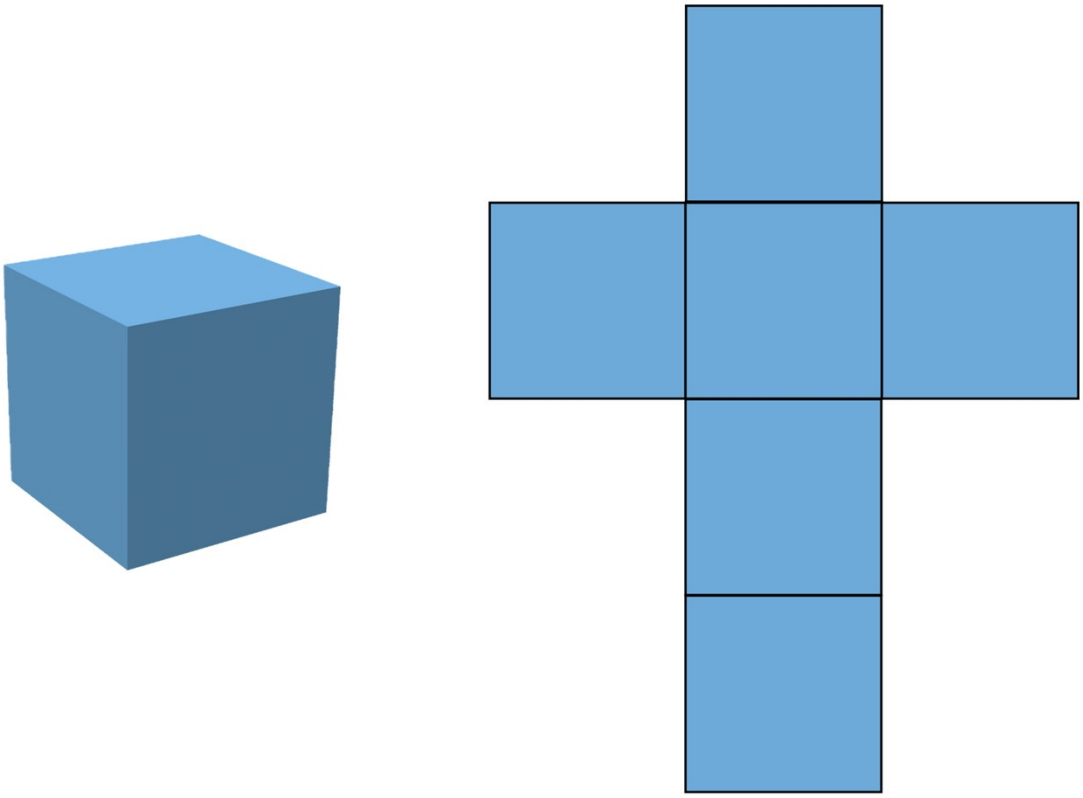

Fig. S3. The schematic and unfolded diagrams of c-Cu_2O.

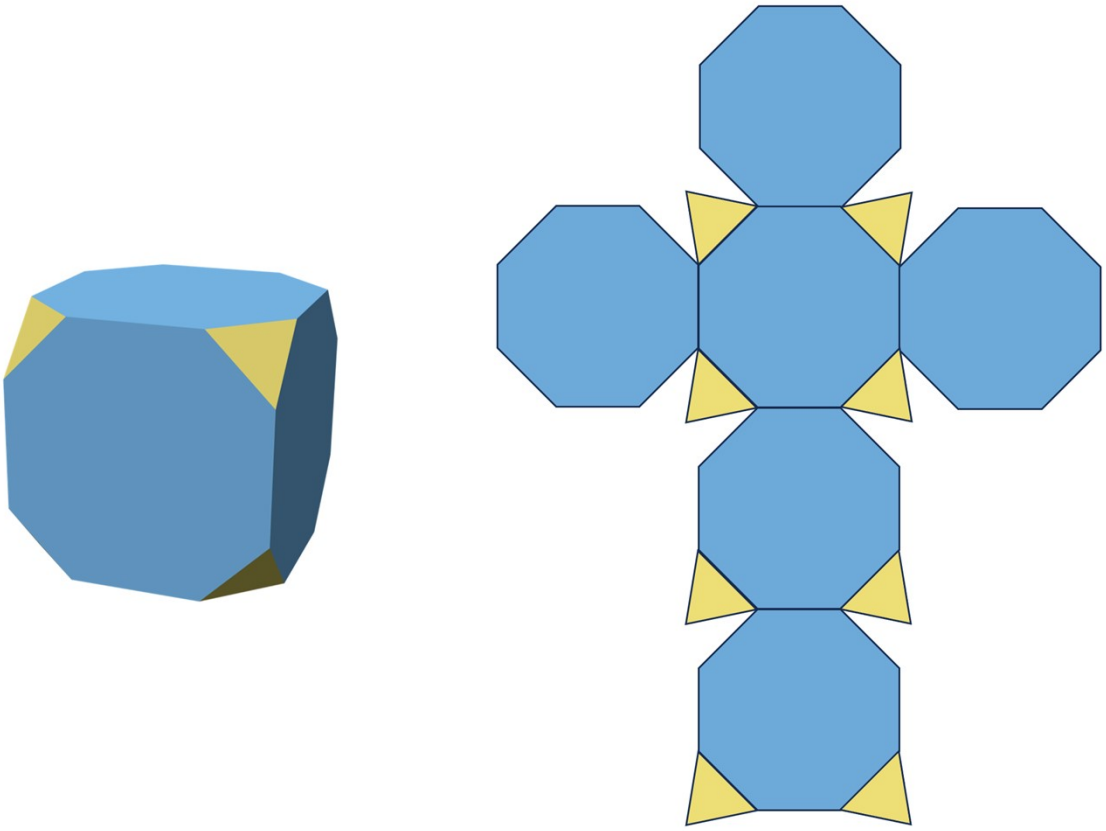

Fig. S4. The schematic and unfolded diagrams of t_1-Cu_2O.

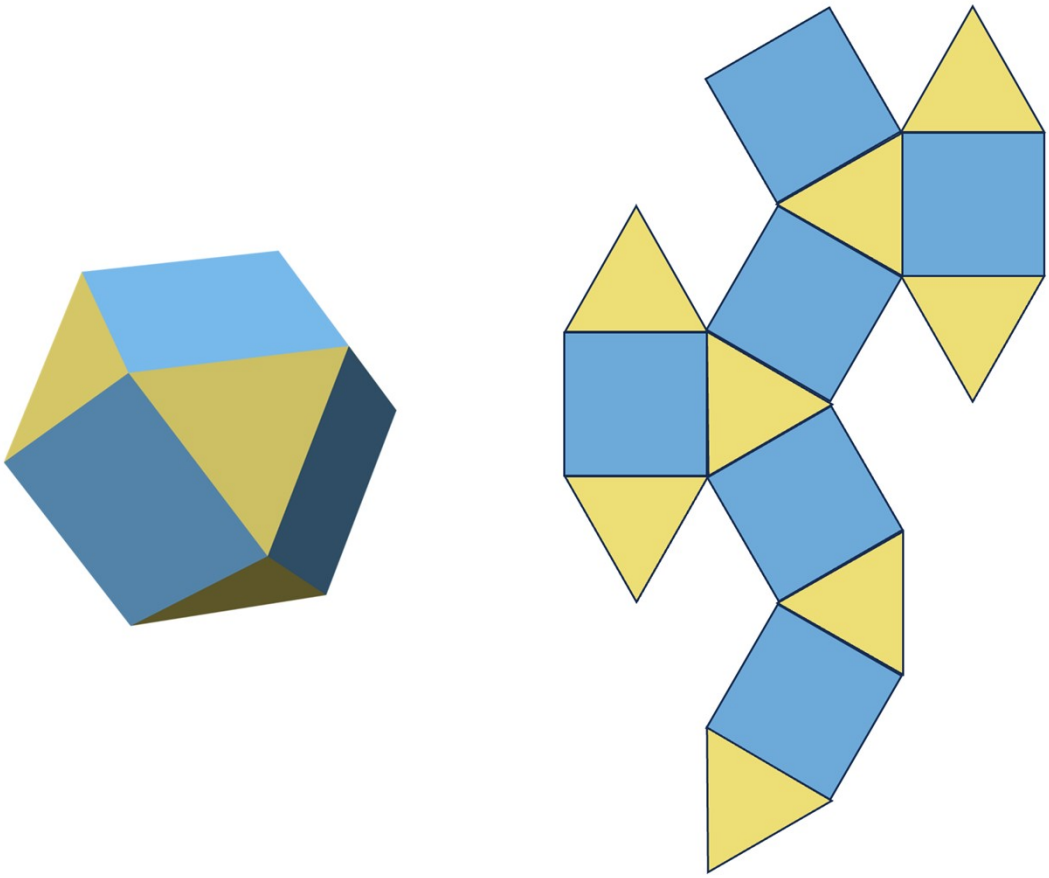

Fig. S5. The schematic and unfolded diagrams of t_2-Cu_2O.

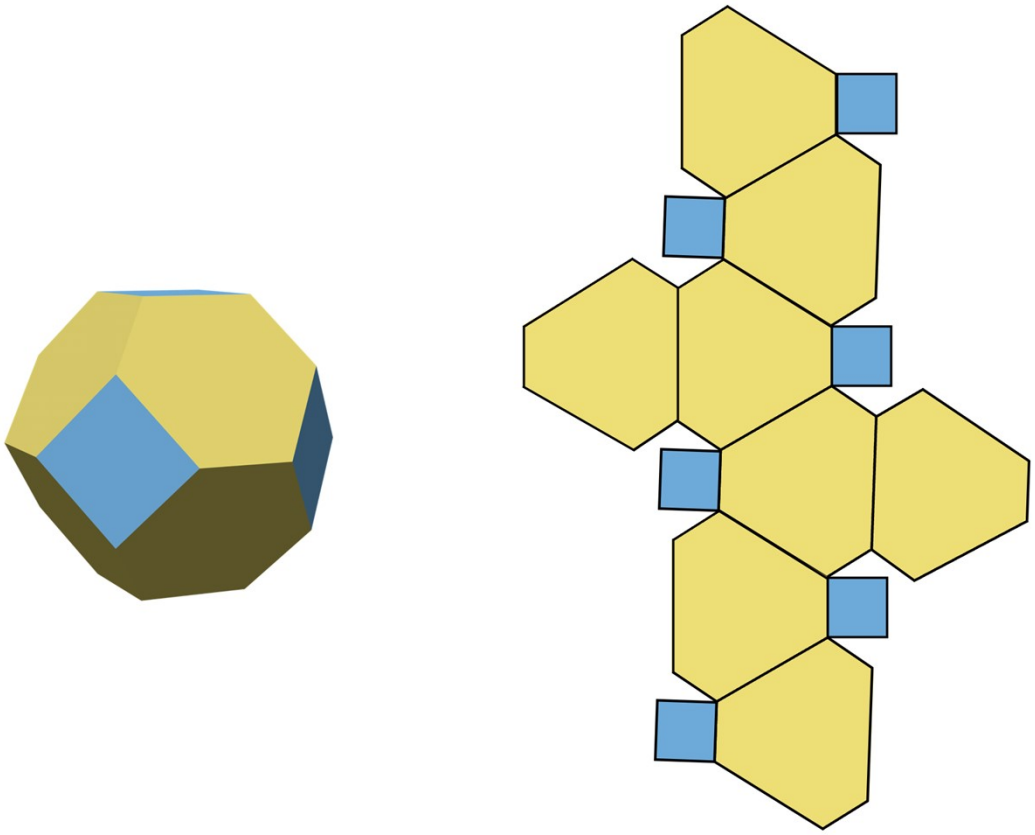

Fig. S6. The schematic and unfolded diagrams of t_3-Cu_2O.

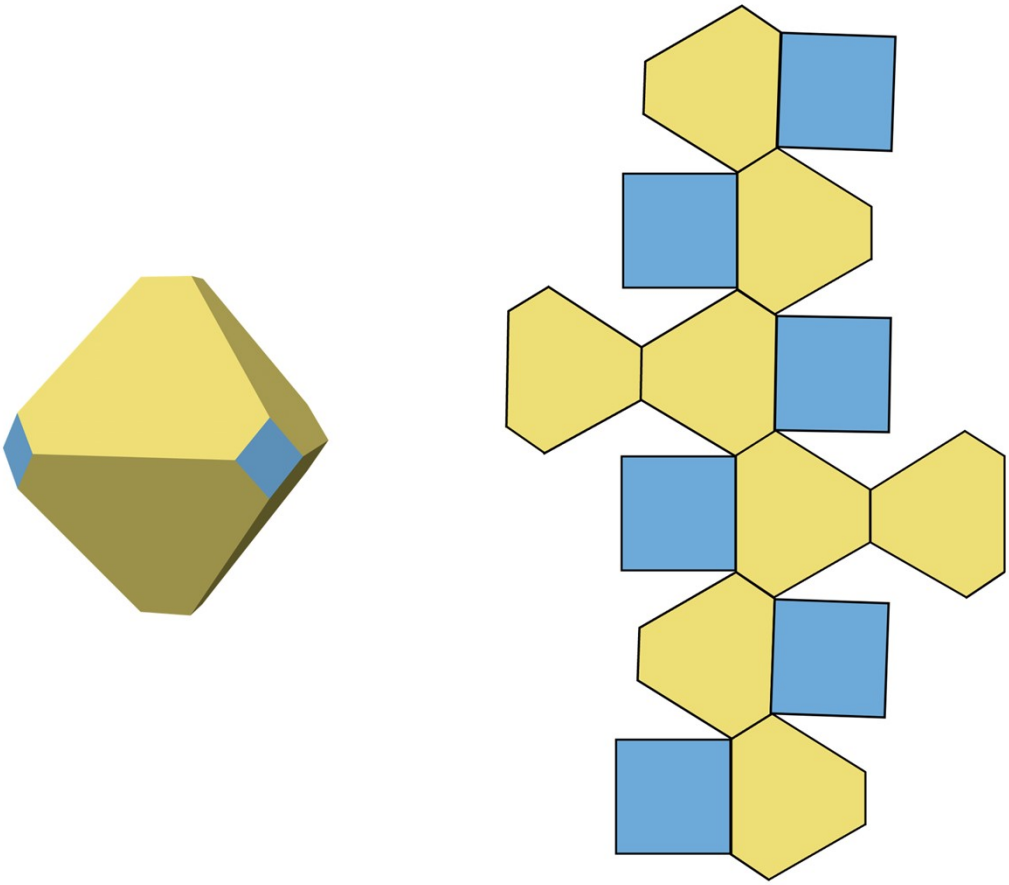

Fig. S7. The schematic and unfolded diagrams of t_4-Cu_2O.

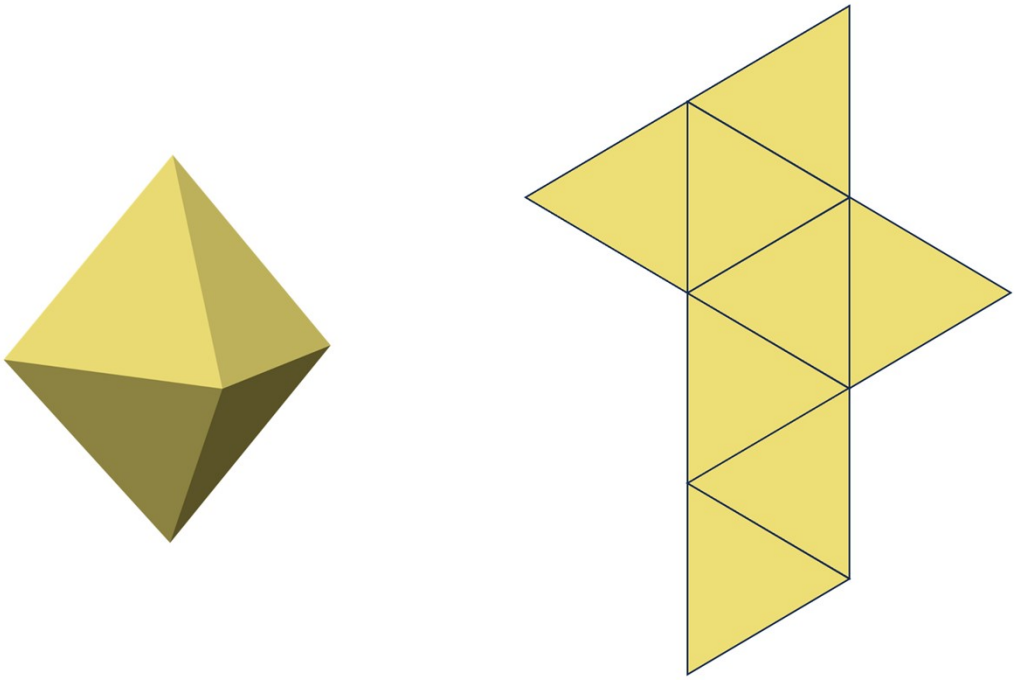

Fig. S8. The schematic and unfolded diagrams of o-Cu_2O.

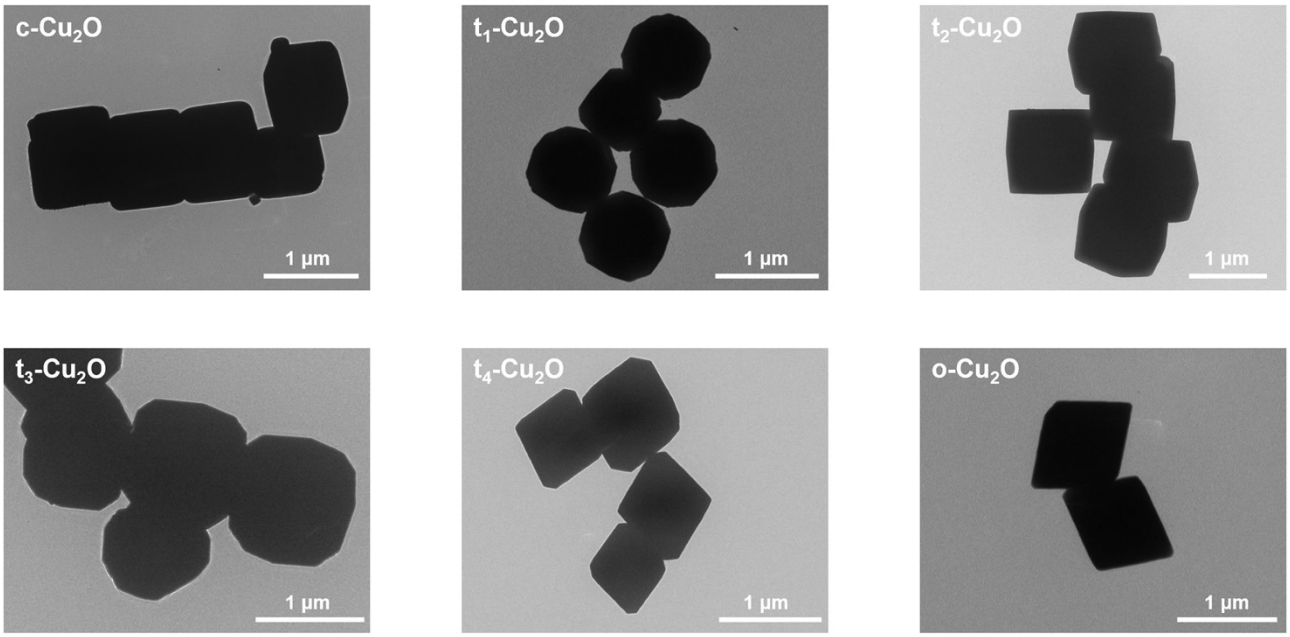

Fig. S9. Low-magnification TEM images of c-Cu_2O, t_{1-4}-Cu_2O, and o-Cu_2O.

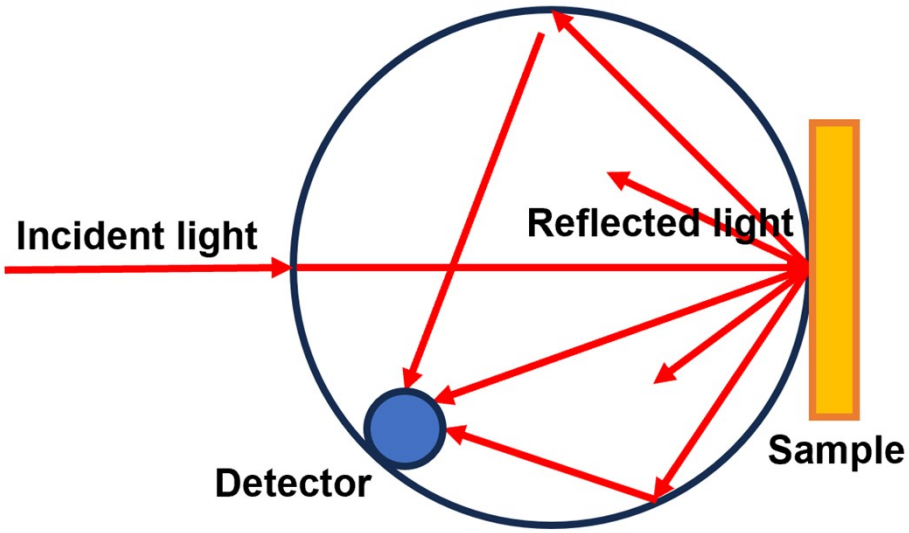

Fig. S10. Optical path diagram of integrating sphere in reflectance mode.

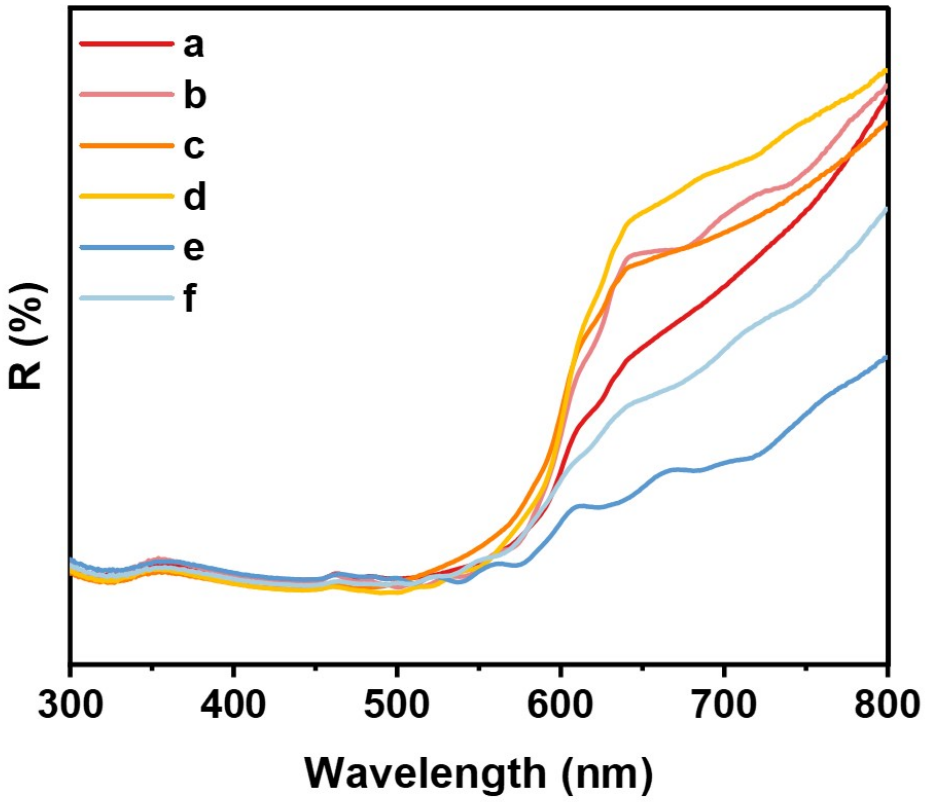

Fig. S11. Reflectance spectra of (a) c-Cu_2O, (b) t_1-Cu_2O, (c) t_2-Cu_2O, (d) t_3-Cu_2O, (e) t_4-Cu_2O, and (f) o-Cu_2O.

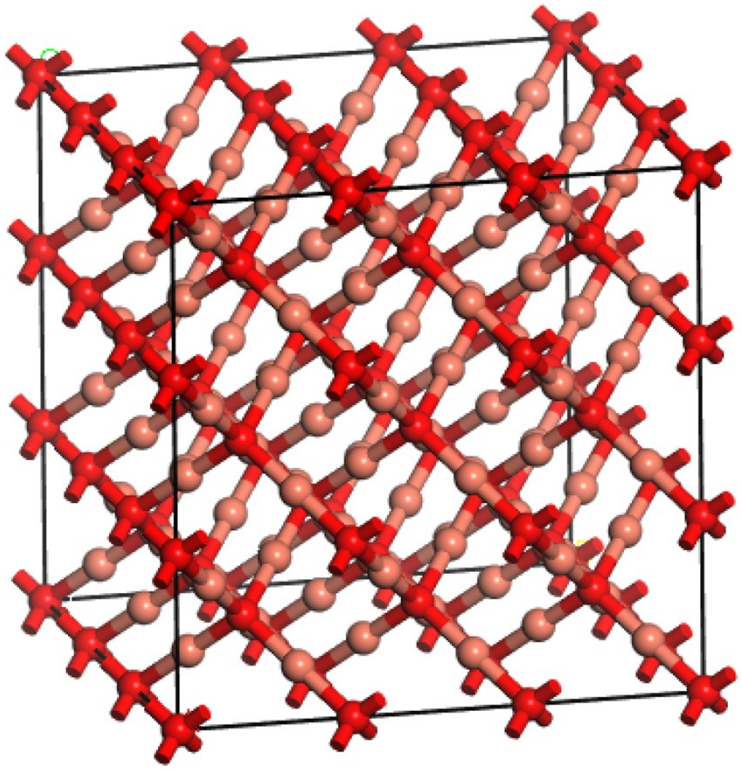

Fig. S12. Geometrically optimized models for Cu_2O bulk.

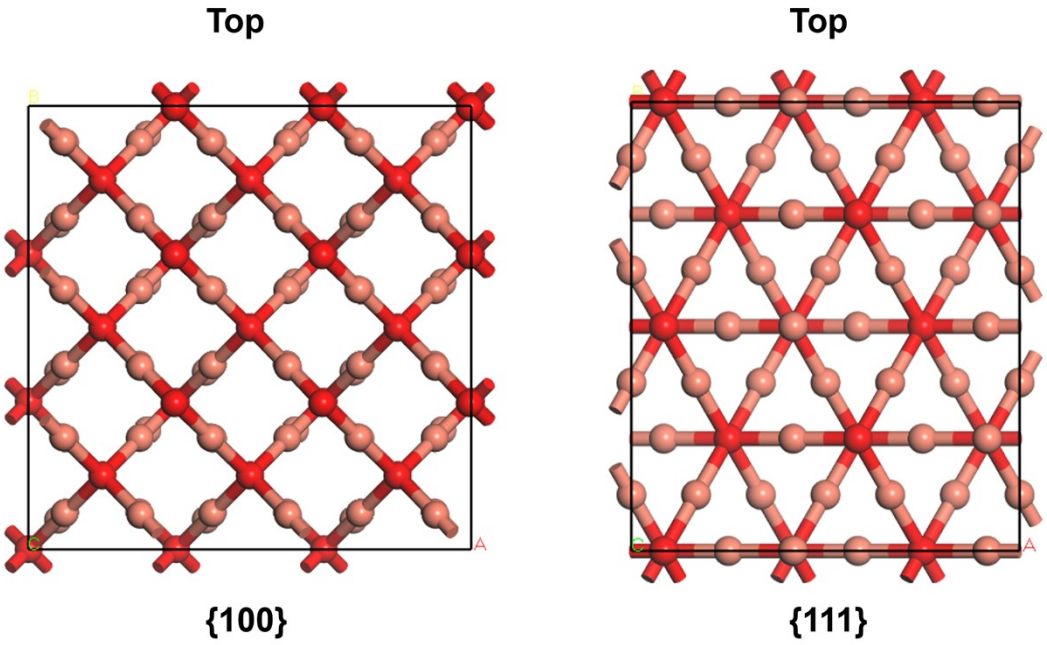

Fig. S13. Top view of the optimized structures of Cu_2O {100} and {111} crystal facets.

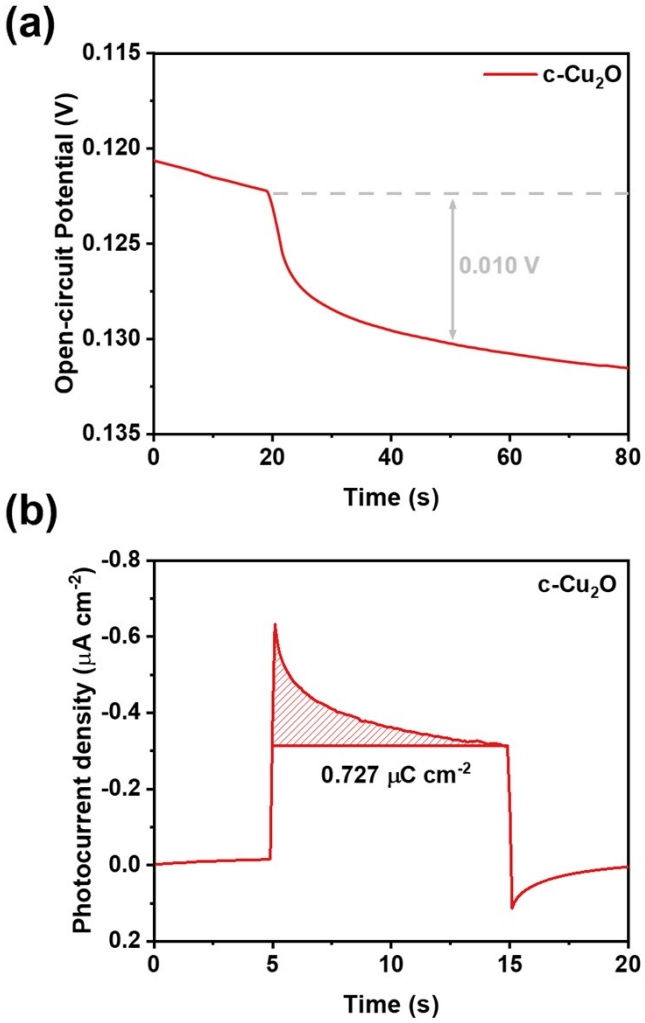

Fig. S14. (a) Surface voltage and (b) transient photocurrent density of c-Cu_2O.

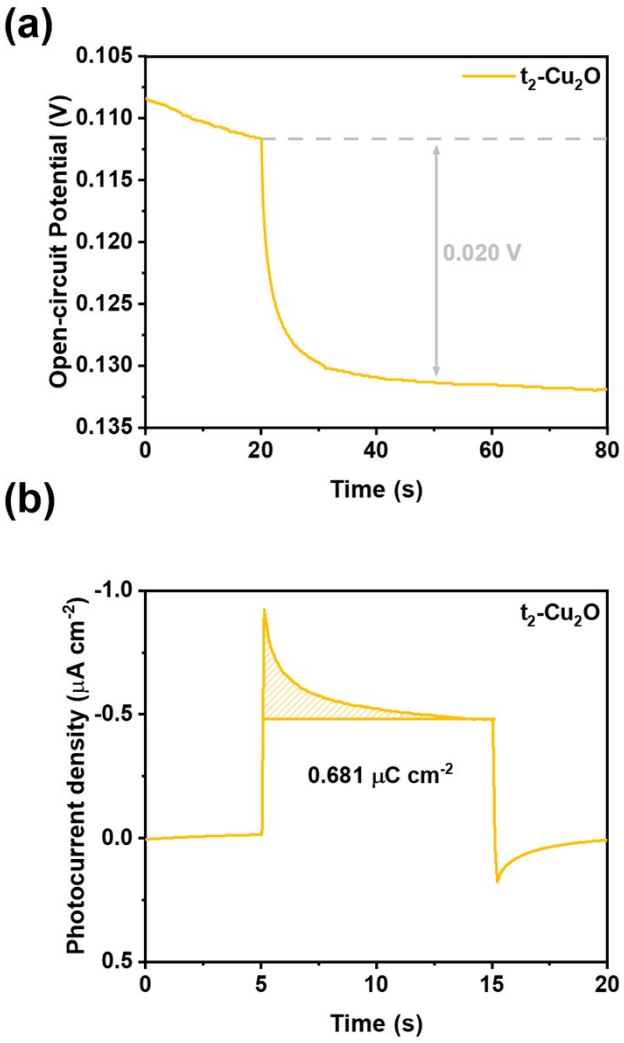

Fig. S15. (a) Surface voltage and (b) transient photocurrent density of t_2-Cu_2O.

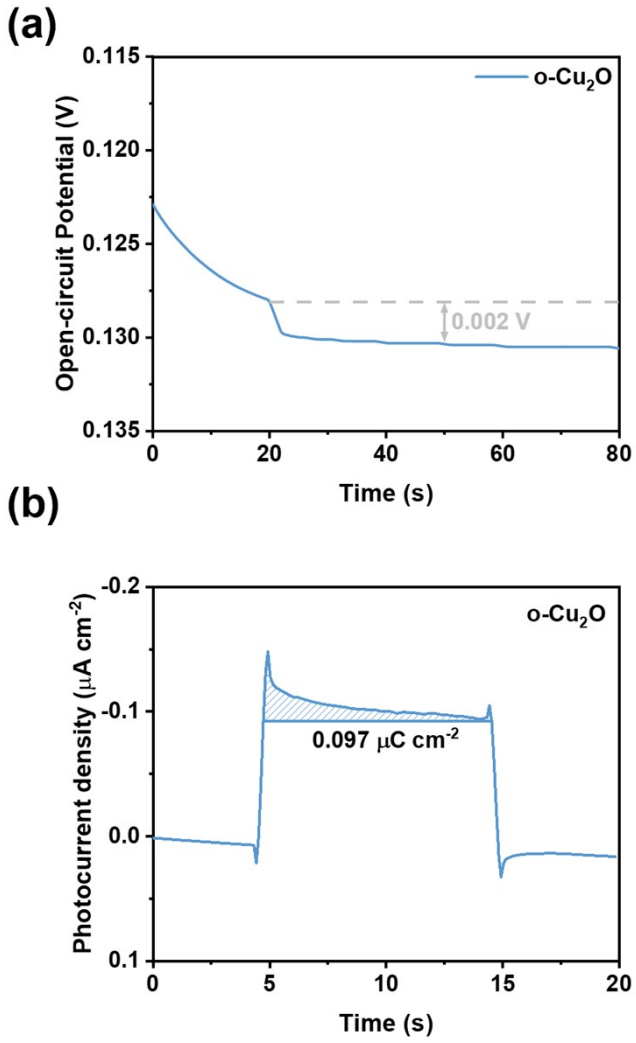

Fig. S16. (a) Surface voltage and (b) transient photocurrent density of o-Cu_2O.

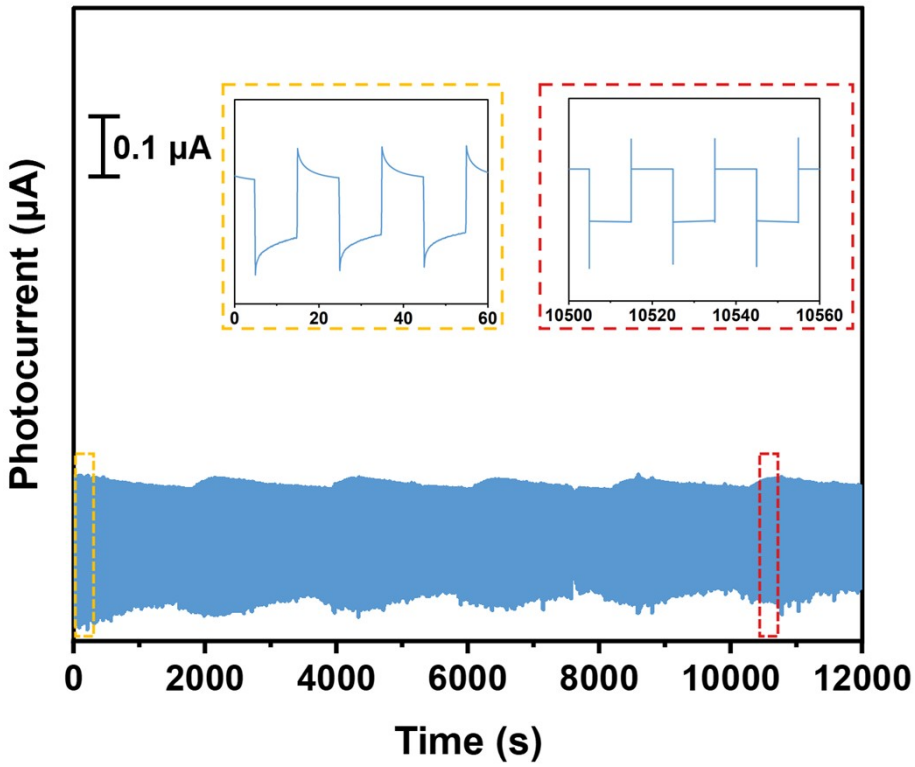

Fig. S17. Long-term cycling stability testing of the PEC biosensor under conditions of 25 ng mL^{-1} CEA.

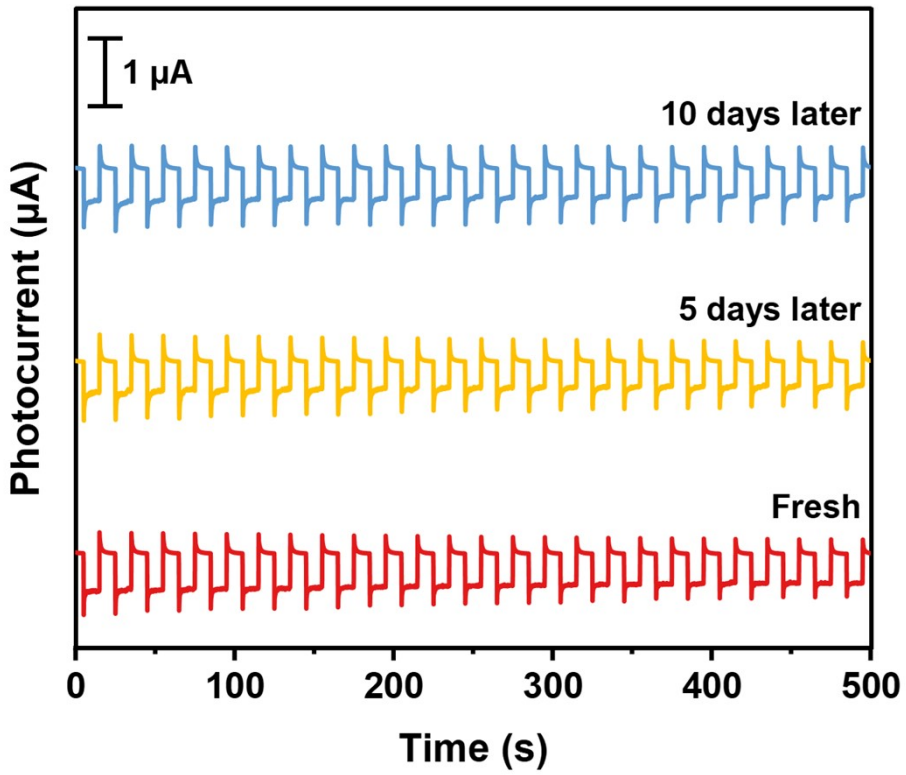

Fig. S18. Time stability test of t_2-Cu_2O photoelectrode with time duration of 5 days and 10 days.

Table S1. The optical power densities for each wavelength.

Wavelength (nm)	400	450	500	550	600	650
$P_{\lambda-in}$ (mW cm^{-2})	0.2964	0.2632	0.2374	0.1988	0.1534	0.1140

Table S2. Comparison of PEC performance of recent reported Cu_2O-based photoelectrodes.

No.	Photoelectrodes	Photocurrent (μA)	Bias voltage	E_g (eV)	Ref.
1	H-Cu_2O/GCE	0.132	-0.1 V vs. Ag/AgCl	1.94	[8]
2	Cu_2O@Ni foam	-0.400	0 V vs. Ag/AgCl	2.10	[9]
3	IL-Cu@Cu_2O	-0.385	0 V vs. Hg/$HgCl_2$	1.98	[10]
4	Cu_2O	0.150	0 V vs. Ag/AgCl	2.27	[11]
5	t_2-Cu_2O/FTO	-0.925	0 V vs. Ag/AgCl	1.95	This work

Table S3. Comparison of the PEC biosensor prepared in this study with other reported methods for determining CEA.

No.	Method	Response range (ng mL^{-1})	LOD (ng mL^{-1})	Ref.
1	Fluorescent lateral flow immunoassay	1 – 320	0.37	[12]
2	Gas-mediated fluorescence immunoassay	0.6 - 20	0.078	[13]
3	Colorimetric aptasensing strategy	4 - 25	0.19	[14]
4	Nanopore-based strategy	2 - 200	0.6	[15]
5	photoelectrochemical	0.1 - 50	58	[16]
6	photoelectrochemical	0.01 - 50	9.31×10^{-3}	This work

Table S4. Comparison of the analytical results between the PEC immunoassay and the commercial CEA ELISA kit in human serum samples.

Sample no.	Method accuracy [Conc.: mean ± SD (RSD), ng mL^{-1}, n = 3]		t_{exp}
	PEC immunoassay	CEA ELISA	
1	2.62 ± 0.17 (6.49%)	2.73 ± 0.21 (7.69%)	0.71
2	16.17 ± 1.41 (8.72%)	18.32 ± 1.33 (7.26%)	1.92
3	7.96± 0.74 (9.30%)	7.68 ± 0.67 (8.72%)	0.49
4	39.52 ± 1.75 (4.43%)	36.48 ± 1.56 (4.28%)	2.25
5	12.85 ± 1.12 (8.72%)	11.54 ± 0.93 (8.06%)	1.56
6	19.37 ± 1.72 (8.88%)	22.41 ± 1.36 (6.07%)	2.40

References

[1] K. Ullah, L. Zhu, Z. Meng, S. Ye, Q. Sun, W. Oh, *Chem. Eng. J.* **2013**, 231, 76.

[2] S. Khan, J. Steffy, M. Safa, H. AL-Shwaiman, V. Subhiksha, A. Syed, L. Wong, M. Verma, *Colloids Surf., A* **2025**, 727, 138214.

[3] X. Zhu, Y. Jia, Y. Liu, J. Xu, H. He, S. Wang, Y. Shao, Y. Zhai, Y. Zhu, *Angew. Chem., Int. Ed.* **2024**, *63*, e202405962.

[4] G. Kresse, J. Furthmüller, *Phys. Rev. B* **1996**, *54*, 11169.

[5] G. Kresse, J. Hafner, *Phys. Rev. B* **1993**, *47*, 558.

[6] Z. Yu, H. Gong, Y. Gao, L. Li, F. Xue, Y. Zeng, M. Li, X. Liu, D. Tang, *Small* **2022**, *18*, 2202564.

[7] Z. Yu, H. Gong, M. Li, D. Tang, *Biosens. Bioelectron.* **2022**, *218*, 114751.

[8] C. Wang, J. Chen, L. Zhang, Y. Yang, M. Huang, C. Chen, C. Li, Y. Xie, P. Zhao, J. Fei, *Carbon* **2022**, 198, 101.

[9] Y. Zhu, Y. Liu, Y. Xu, Y. Ruan, G. Fan, W. Zhao, J. Xu, H. Chen, *ACS Appl. Mater. Interfaces* **2019**, 11, 25702.

[10] J. Li, H. Wang, M. Liu, Y. Qin, Q. Fang, R. Tan, L. Hu, W. Gu, C. Zhu, *Anal. Chem.* **2023**, 95, 10044.

[11] C. Ma, D. Jiang, L. Zeng, Y. Zhou, N. Xu, M. Yang, L. Zhu, X. Xu, *Sens. Actuators B Chem.* **2025**, 445, 138575.

[12] Z. Song, Y. Suo, S. Duan, S. Zhang, L. Liu, B. Chen, Z. Cheng, *Biosens. Bioelectron.* **2023**, *224*, 115063.

[13] S. Liu, D. Lin, Y. Lai, L. Hou, T. Lin, S. Zhao, *Anal. Chem.* **2022**, *94*, 18074.

[14] L. Yang, M. Cui, Y. Zhang, L. Jiang, H. Liu, Z. Liu, *Sens. Actuators B Chem.* **2022**, *350*, 130857.

[15] H. Tang, H. Wang, C. Yang, D. Zhao, Y. Qian, Y. Li, *Anal. Chem.* **2020**, *92*, 3042.

[16] P. Song, M. Wang, Y. Duan, A. Wang, Y. Xue, L. Mei, J. Feng, *Microchim Acta* **2023**, *190*, 85.